Article

Machine Learning for Prediction of Energy in Wheat Production

Ali Mostafaeipour [1,2,3], Mohammad Bagher Fakhrzad [4], Sajad Gharaat [4], Mehdi Jahangiri [5], Joshuva Arockia Dhanraj [6], Shahab S. Band [7,*], Alibek Issakhov [8] and Amir Mosavi [9,10,11,12,*]

[1] Institute of Research and Development, Duy Tan University, Da Nang 550000, Vietnam; alimostafaeipour@duytan.edu.vn
[2] The Faculty of Civil Engineering, Duy Tan University, Da Nang 550000, Vietnam
[3] Department of Sustainable Energy, Faculty of Environmental Management, Prince of Songkla University, Songkhla 90110, Thailand
[4] Industrial Engineering Department, Yazd University, Yazd 89195-741, Iran; mfakhrzad@yazd.ac.ir (M.B.F.); sajadgharaat68@gmail.com (S.G.)
[5] Department of Mechanical Engineering, Shahrekord Branch, Islamic Azad University, Shahrekord 8813733395, Iran; jahangiri.m@iaushk.ac.ir
[6] Centre for Automation & Robotics (ANRO), Department of Mechanical Engineering, Hindustan Institute of Technology and Science, Chennai 603103, India; joshuva1991@gmail.com
[7] Future Technology Research Center, College of Future, National Yunlin University of Science and Technology 123 University Road, Section 3, Douliou, Yunlin 64002, Taiwan
[8] Faculty of Mechanics and Mathematics, Department of Mathematical and Computer Modelling, Al-Farabi Kazakh National University, Almaty 050040, Kazakhstan; Alibek.issakhov@kaznu.kz
[9] Faculty of Civil Engineering, Technische Universität Dresden, 01069 Dresden, Germany
[10] School of Economics and Business, Norwegian University of Life Sciences, 1430 Ås, Norway
[11] Kando Kalman Faculty of Electrical Engineering, Obuda University, 1034 Budapest, Hungary
[12] Thuringian Institute of Sustainability and Climate Protection, 07743 Jena, Germany
* Correspondence: shamshirbands@yuntech.edu.tw (S.S.B.); amir.mosavi@mailbox.tu-dresden.de (A.M.)

check for updates

Abstract: The global population growth has led to a considerable rise in demand for wheat. Today, the amount of energy consumption in agriculture has also increased due to the need for sufficient food for the growing population. Thus, agricultural policymakers in most countries rely on prediction models to influence food security policies. This research aims to predict and reduce the amount of energy consumption in wheat production. Data were collected from the farms of Estahban city in Fars province of Iran by the Jihad Agricultural Department's experts for 20 years from 1994 to 2013. In this study, a novel prediction method based on consumed energy in the production period is proposed. The model is developed based on artificial intelligence to forecast the output energy in wheat production and uses extreme learning machine (ELM) and support vector regression (SVR). In the experimental stage, the value of elevation metrics for the EVM and ELM was reported to be equal to 0.000000409 and 0.9531, respectively. Total input energy (consumed) is found to be 1,460,503.1 Mega Joules (MJ), and output energy (produced wheat) is 1,401,011.945 MJ for the Estahban. The result indicates the superiority of the ELM model to enhance the decisions of the agricultural policymakers.

Keywords: wheat production; extreme learning machine (ELM); machine learning; support vector regression (SVR); food science; data science; big data; network science; artificial intelligence; artificial neural network

1. Introduction

The adverse effects of population growth on food resources have been studied in several studies [1]. Food security has become more than ever a national security matter of various countries worldwide [2]. The food and agriculture organization (FAO) also emphasizes food security as a measure to facilitate the access of all people to sufficient, safe, and nutritious food to satisfy dietary needs and appetite preferences for an active and healthy life. With regard to this definition, agricultural policymakers must ensure that there is enough food for the communities' dietary needs [3]. Therefore, they should pay more attention to foodstuff forecasting methods [4]. In 2013, the total harvested area was 218.4, the average yield was 3264 kg per hectare, and the total wheat production was equal to 713 million tons. Wheat is an essential plant in Iran, with more than 50% of entire arable lands allocated to it [5]. Thus, in-depth insight into the production and energy usage are of utmost importance for food security and energy planning.

Global wheat crop condition, mostly favorable provided by the Agricultural Market Information System (AMIS) [6], shows that the European Union ranks first followed by China and India, regarding wheat production. Table 1 represents the global wheat production and its projection in a million tons. It shows that EU ranks first, following by China, India, and USA, respectively [7].

Table 1. Information of the production and forecast of wheat all over the world in a million tons.

Country	Average of 5 Years	2018 Estim	2019 Fcast
EU	150.3	137.5	149.0
China Mainland	129.2	128.0	129.0
India	94.6	99.7	99.0
USA	54.6	51.3	52.0
Russia	70.5	72.1	79.0
Australia	23.3	17.3	24.0
Canada	30.2	31.8	33.0
Pakistan	25.8	25.5	24.5
Turkey	20.7	20.0	21.0
Ukraine	25.5	24.6	26.5
Kazakhstan	14.1	13.9	14.5
Iran	11.8	13.4	11.4
Argentina	16.3	19.5	19.0
Egypt	9.2	8.8	9.0
Uzbekistan	6.6	6.0	6.5
Others	59.6	59.0	58.0
World	742.3	728.3	757.4

The total area under wheat cultivation in the 2014 crop year was reported to be 6.4 million hectares. The total wheat harvest of the country was 12 million tons. Eight million tons of this amount was irrigated wheat. The average yield of irrigated wheat is 3.5 tons per hectare [8]. In 2015, the total cultivated area for wheat was estimated to be 5.7 million hectares. The country produces about 11.5 million tons of wheat. Fars is the second-highest wheat-producing province with 10.19% of Iran's total wheat production. Irrigated wheat yields an average of 3993.2 kg per hectare in Fars from 2015 to 2016. Agricultural policymakers in Iran believe that the exact amount of wheat production in the country must be assessed. Importing excess wheat leads to a price reduction in the country. This can decrease farmers' profits or even cause them to be looser. On the other hand, insufficient wheat imports can lead to unmet demands and an increase in the wheat price, so people cannot afford their annual wheat costs. Engineers in various fields are interested in analyzing current and past data for future predictions using a variety of techniques, such as statistics, modeling, time series, and learning machines.

With each publishing, a variety of crop status maps are produced and distributed. A propagation map showing crop conditions in the major wheat-growing areas was created at the Commission's

request. A visual summary of global AMIS crop conditions for the study is now accessible in the area of the wheat production chart (Figure 1). The standalone crop report and the website provide further crop-specific and seasonal maps. Figure 1 provides information about the wheat-growing location in Iran, adapted from [9]. It shows that Khorasan Province in the northeast and Fars Province is the south of Iran are significant locations for wheat production.
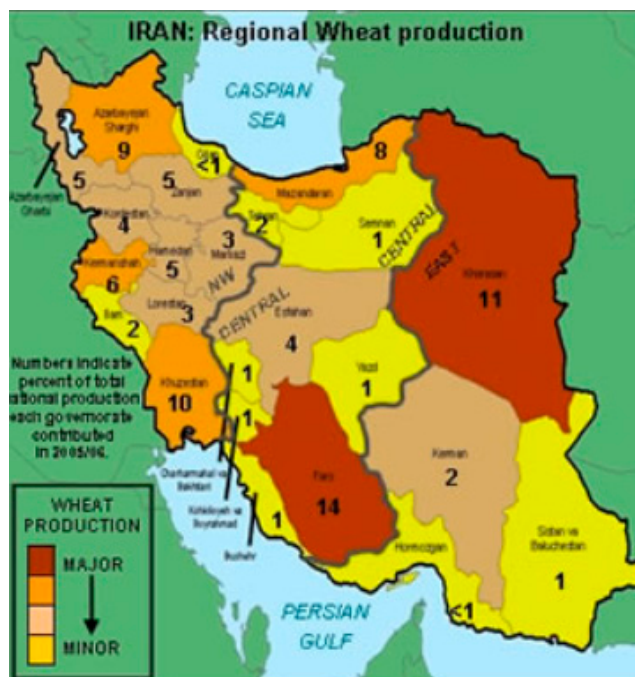

Figure 1. Information about the agricultural land and wheat growing location in Iran.

Table 2 shows the overall wheat and other main productions like barley and rice in Iran. The wheat import from Iran has been decreasing since 2014 dramatically [10,11].

Table 2. Overall wheat production in Iran in 1000 tones for Iran.

Cereal Production	2014–2018 Average	2018	2019 Forecast	Change 2019/2018
Wheat	11,820	13,400	13,400	0.0
Barley	2993	2800	3000	7.1
Rice (paddy)	2737	3020	3020	0.0
Others	1239	914	1125	22.0
Total	18,789	18,789	20,535	2.0

The main goal of this study was to predict the total amount of required energy for wheat production. For this purpose, city of Estahban in Fars Province of Iran was nominated as the case study. This research's contribution is that the ELM and SVR methods are used as methods to forecast energy output to determine the best method with the least forecast error for prediction of energy in wheat production of the Iranian city of Estabhan for the first time. Another contribution that highlights this research is the selected seven *Input* data used for analyzing the methods.

In Section 2, a literature review is presented. In Section 3, the materials and methods are discussed. Results and discussion are presented in Section 4. Finally, Section 5 is the conclusion.

Literature Review

In recent years, many researchers have analyzed the energy consumption for producing agricultural products. In the past 15 years, neural networks have attracted considerable attention. Artificial neural

network (ANN) models are based on the biological activities of neurons. Biological neural networks have turned into a critical modeling technique that is used more than other complex input-output methods. ANNs are good for some tasks but not for others. They can learn from examples and solve nonlinear problems (support vector regression) [12]. The support vector machine (SVM) method was considered better than ANN in late 1990, because it gave attractive and better solutions in problems. SVR theory is developed from computational theory, but the development in ANNS is more heuristic. While ANNs minimize empirical risk or training error, SVMs minimize structural risk. In SVR, the objective function is convex, so the global optimum is always reached [13]. SVM is used for discrete data, and SVR is used for continuous data [14]. In a study by Hosseinzadeh-Bandbafha et al. [4] on energy consumption and efficiency in dairy farms in Qazvin, Iran, they estimated the greenhouse gas emissions due to energy consumption in these farms and attempted to optimize the energy use of the farms to reduce the emission rate and the total emission produced. Memon et al. [15] studied the energy consumption pattern in wheat production in Pakistan and concluded that wheat cultivation achieved the highest net energy.

In a study by Zangeneh et al. [16] on potato production units' energy consumption in Hamadan, Iran, these units' energy consumption was determined through in-person interviews with 100 farmers. The farmers were divided into 1: 68 farmers with a high farming machinery level, and 2: consisting of 32 farmers with a low level of farming technology and without machinery. The researchers concluded that farming machinery is necessary to improve the amount of potato production regarding the benefit to cost ratio. Proximal support vector machine (PSVM) and least square support vector machine (LS-SVM) models are derived from SVM that have a higher speed.

Single hidden layer feedforward neural networks (SLFNs) are learning platforms that can widely use feature mappings [17]. ELM is a complex learning algorithm for SLFNs, randomly selecting the input weights matrix and the hidden layer biases [18]. Neumann et al. [19] showed that ELM is appropriate for this purpose.

Nath et al. [20] published an autoregressive integrated moving average (ARIMA) simulation method analysis on the estimation of wheat production in India. The wheat production in India was projected with a time series simulation method. The optimal ARIMA configuration for the analysis was identified to be ARIMA (1, 1,0). The goal was to predict future wheat production by adapting ARIMA (1,1.0) to our time series data for up to 10 years as accurately as possible. The outcomes of the forecasts suggest that the annual production in 2026 and 2027 would increase. With an estimated annual growth rate of about 4%, wheat production will continue to grow. The long short-term memory (LSTM) neuronal network forecasting model for wheat production in Pakistan was reported by Haider et al. [21]. This paper is concerned with creating an effective wheat production prediction model utilizing neural networks with the use of (LSTM). In combination with the LSTM model, a smoothing data preprocessing method is used to enhance predictive precision further. Santamaría-Artigas et al. [22] carried out an evaluation of the near-surface air temperatures arising from the US and Ukraine's reanalysis. This paper analyses ERA-Interim (ERAI), Japanese 55-year reanalysis, Modern-Era Research and Development Retrospective Analysis Version 2, and NCEP1 and NCEP2 reanalysis works for near-surface air sites. The re-analysis data were first related to measurements from weather stations in the US and Ukraine and then analyzed within a winter wheat yield model. The data was validated in the United States and Ukraine. The evaluation of the weather station results indicated that all the data samples worked properly ($r2 > 0.95$) and more recent re-analysis, like ERAI, had smaller root-mean-square deviation (RMSD ~0.9 °C) errors relative to traditional high-resolution datasets, such as NCEP1 (RMSD ~2.4 °C).

The multi-scale and multi-model gridded method for assessing crop production, risk analysis, and impact studies on climate change was introduced by Shelia et al. [23]. This paper provides an overview of gridded crop models and yield forecasts, together with risk analysis and climate impact analyses, methods, techniques, prototypes, and capabilities for the CCAFS Regional Agricultural Forecasting Toolbox (CRAFT). Yazdani [24] completed an economic and scientific evaluation of environmental components in Tabriz and Isfahan (Iran). In this analysis, various climatic variables,

including temperature, precipitation, and freezing, were measured to determine the economic value of the environment. For the Tabriz and Isfahan agriculture areas, four products were selected, namely arable wheat, dry farm wheat, arable barley, and dry farm barley. Ram et al. [25] examined health identification of wheat crop utilizing pattern recognition and image processing. The writers came to incorporate a form of pattern identification and an approach of image processing. The system allows a farmer to adopt a particular crop trend in order to assess risks sooner. Combining it with the power of the Internet of Things (IoT), individuals without the need of human resources will simplify the process. Ultimately, this work will speed up farming and enable farmers to grow more in less time.

In a study by Ali and Deo [26], the wheat yield was modeled by a data-intelligent algorithm based on the artificial neural network and genetic programming and minimax probability machine regression (MPMR) results were compared. The criteria used for this comparison were correlation (*r*), Willmott's index (*WI*), Nash–Sutcliffe coefficient (*EV*), root-mean-square error (*RMSE*), and mean absolute error (*MAE*). The *r, WI,* and *EV* values obtained for station 1 were as follows: for the ANN model, $r \approx 0.983$, $WI \approx 0.984$, and $EV \approx 0.962$; for the MPMR model, $r \approx 0.957$, $WI \approx 0.544$, and $EV \approx 0.527$; and for the genetic programming (GP) model, $r \approx 0.982$, $WI \approx 0.980$, and $EV \approx 0.955$. The *RMSE* and *MAE* values obtained for the optimal ANN model ($RMSE \approx 192.02$; $MAE \approx 162.75$) were lower than those for the MPMR model (614.46 kg/ha; $MAE \approx 431.29$ kg/ha) and for the GP model ($RMSE \approx 209.25$ kg/ha; $MAE \approx 182.84$ kg/ha). For both stations, ANN outperformed GP and MPMR in terms of RMSE and MAE and the Legates–McCabe index (*LM*). These results demonstrated the excellent capability of ANN as a data-intelligent algorithm in the forecasting of wheat yield based on the nearest neighbor scheme. Salim and Raza [27] conducted a study of the sustainable wheat production nutrient use efficiency (NUE) research. Kamir et al. [28] did a study on forecasting wheat yields in Australia using weather data, time series for satellite images, and machine learning processes. The machine-learning regression models also showed superior performance compared to the methods based on peak normalized difference vegetation index (NDVI) and harvest index ($R^2 < 0.46$).

Pantazi et al. [29] introduced three based models, of supervised Kohonen networks (SKNs), counter-propagation artificial networks (CP-ANNs), and XY-fusion (XY-F) that implement supervised learning for associating high-resolution data on soil and crop, which utilized iso-frequency classes of yield productivity for wheat. They concluded that the SKN model had better accuracy for prediction. Amato et al. [30] introduced a novel multimedia summarization model from online social networks (OSNs). They focused on the management and sharing of multimedia information. They proposed the summary of the model and heuristics to get a multimedia summary with priority, continuity, variety, and not repetitive features. The results were also validated. Wang et al. [31] carried out efforts to improve the surface energy balance network's meteorological feedback using the mesoscale environment analysis and prevision model. Comparisons of data collected at the weather station were carried out to determine the quality of weather research and forecasting (WRF) simulation. The results showed high agreement between the reports of meteorological stations and wind speed ($R^2 = 0.628$), air temperature ($R^2 = 0.8242$), relative humidity ($R^2 = 0.8089$), and surface pressure ($R^2 = 0.8915$) values obtained from WRF. According to the above notions, this study aimed to improve the accuracy of the amount of wheat production forecast in Estahban using energy input. The exact forecasting of the harvested amount at the end of the harvest season is essential for import or export planning by policymakers in this field. We used SVR and ELM methods to forecast the wheat yield. Consequently, the research questions are as follows.

1. How much energy is required to produce wheat in Estahban?
2. Is it efficient to produce wheat regarding energy consumption?
3. Which method has higher accuracy for prediction?

2. Materials and Methods

2.1. Data Collection and Processing

Fars ranks the second wheat-producing province in Iran, with 10.19% of the country's total wheat production. The yield of irrigated wheat in Fars is equal to 2.3993 kg/hectares [8]. The Estahban town, with an elevation of 1690 m above the sea level and annual precipitation of between 50 and 450 mm, has an average yearly temperature of Celsius degrees (Organization for Research and Planning). Figure 2 shows the geographic location of the studied area.

The data for this research were obtained from agricultural experts and engineers in the area of Estahban town, as well as the selected farmers in the region. Data were collected from the farms of Estahban city in Fars province by the Jihad Agricultural Department experts during 20 years from 1994 to 2013. Out of 145 farms, 105 farms were selected as the sample size (Cochran's formula). All 105 farms in the Estahban region had the same climate and geographical characteristics and a mechanized agricultural system.

This study's energy analysis aimed to estimate the energy equivalent of inputs and outputs in wheat production. The information for wheat production consists of grains, water, different kinds of fertilizers, pesticides, labor, equipment, machinery, and gasoline [32].

The inputs and outputs have different units. For example, the unit for measurement of diesel fuel is a liter, while chemical substances are measured with their mass (kilograms). In the present study, the energy equivalent (MJ ha^{-1}) was used to convert all inputs and outputs into the same unit. Table 3 shows that such unit conversion is common for determining the agricultural studies' input and output flows. To obtain the energy equivalent of inputs, the input rate is multiplied by the corresponding energy coefficient [32].

Table 3. Energy conversion data.

Input/Output	Unit	Energy Equivalent (MJ/h)	Reference
Input			
1- Consumed water	M^3	1.02	[33]
2- Chemical fertilizers	Kg		
Nitrogen		66.14	[34]
Phosphate		12.55	[34]
Potassium		11.15	[34]
3- Pesticides	Kg		
Decis		120	[35,36]
Carbendazim		120	[35,36]
Pirimor		120	[35,36]
Herbicide		120	
4- Labor	h	1.96	[37]
5- Diesel fuel	L	56.31	[35,38]
6- Equipment and machines	h	62.7	[37]
Prepare Tractor and land			
Fixed equipment			
Tools and machinery			
Combine			
Pesticide Sprayer			
Water pump			
7- Grain	kg	14.7	[39]
Output			
8- Wheat	kg	14.7	[39]

Figure 2. The topographic map of Estahban.

2.2. Selected Input for the Model

The first step in product forecast is the selection of model inputs. The energy input from various sources used in the production process is considered the model input, and the energy output is considered the model output. We used the units in Table 3 to find the energy equivalent of the input and output amounts. All the input and output equations are calculated by the product of the input value and MJ/h [16]. Therefore, we considered 12 agricultural input variables for the model. This study considered different agricultural mechanization indexes, frequency and duration of irrigation, and farm size as input variables to improve the forecast model. The model inputs were determined by the farmers to provide simple measurement and clarity in answers. This study used IBM SPSS version 22 and MATLAB R2013a software.

2.3. Support Vector Machine (SVM)

SVM is a classifier, which belongs to the category of kernel methods of machine learning. The linear decision functions that SVM is looking for are as follows:

$$(x) = (w.\varnothing(x) + b) \tag{1}$$

The distance between two classes (margin) in the transformed feature space is shown as $\frac{2}{\|w\|}$. The SVM model seeks to maximize the margin and minimize the training error. The optimization problem will be as follows.

$$Minimize\ LPrimal - SVM = \frac{1}{2}\|w\|^2 + C\sum_{i=1}^{N}\varepsilon_i \tag{2}$$

subject to:$(w.(xi) + b) \geq 1 - \xi i,\ i = 1,\dots,N,\ \xi i \geq 0\ i = 1,\dots,N.$

where the user-defined parameter C determines the tradeoff between the margin size and training error, and the Xi data in $t_i(w.(x_i) + b) = 1$ is called a support vector.

2.4. Least Square Support Vector Machine (LS-SVM) Model

The LS-SVM model is the least square error model of the SVM. In this model, the training errors are minimized as square errors in the optimization problem and the inequality constraints are changed to equality type constraints. So, it is possible to implement this method solving a set of linear equations, instead of quadratic programming. LS-SVM optimization is as follows:

$$Minimize\ L\ Primal\ -\ LS-SVM\ =\ \frac{1}{2}\|w\|^2 + C \tag{3}$$

subject to: $(w.(xi) + b) = 1 - \xi i\ i = 1, \dots ,N$.

In LS-SVM, the αi values are proportional to the ith data point error, while in SVM, these values are equal to zero for most of the data.

2.5. Proximal Support Vector Machine (PSVM) Model

The mathematical model for PSVM is given by:

$$Minimize\ L\ Primal\ -\ PSVM\ =\ \frac{1}{2}\|w\|^2 +\ b^2 + C\frac{1}{2}\sum_{i=1}^{N}\varepsilon_i^2 \tag{4}$$

subject to: $(w.(x_i) + b) = 1 - \xi i\ i = 1, \dots ,N$.

The distinction between SVM, LS-SVM and PSVM models is how to deal with the training error in the optimization problem. The LS-SVM and PSVM models have changed nonlinear constraints to linear ones by changing the objective function, and thus, are able to solve the new optimization problem faster [40].

2.6. Extreme Learning Machine (ELM)

ELM theory shows that although hidden neurons play an important role in neural algorithms, this role may not necessarily involve iterative tuning of neuron parameters. In fact, it is possible to have an algorithm in which every parameter of a hidden neuron is generated randomly from a continuous probability distribution and completely independent of training samples [41]. Using ELM, it is possible to approximate any continuous function. ELM network structure: The parameters of hidden nodes (a_i, b_i) are randomly generated. $h_i(x) = g(a_i.x.b_i)$ is the ith hidden node's output for input x, where g is a nonlinear piecewise continuous function (Kasun et al., 2016). Figure 3 illustrates a schematic of the neuron network structure.
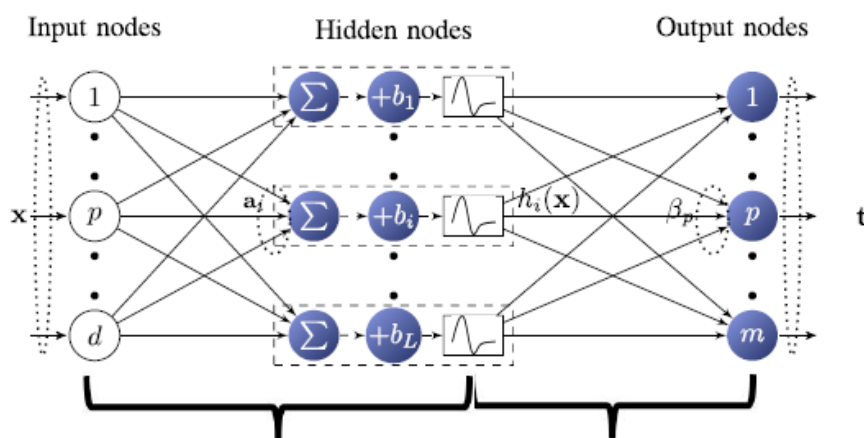

Figure 3. Schematic neuron network structure [42].

The aim of this model is to propose an integrated model that encompasses all SVM, LS-SVM, and PSVM methods. The ELM model was first proposed for SLFNs and then developed for generalized SLFNs. The output function for generalized SLFNs is given by [42,43]:

$$(x) = h(x)\beta = \sum_{i=1}^{L} \beta i h i(x). \tag{5}$$

The $h(x)$ function maps the d-dimensional space of the input into an L-dimensional space. There is a weight between the hidden layer and the output layer. It is argued that if the appropriate mapping is selected in the hidden layer, approximating any function is possible with this model. For a two-class arrangement problem, the decision function according to [42,43], is as follows.

$$(x) = (h(x)\beta). \tag{6}$$

One of the features that differentiate the ELM models from typical learning methods is that they try to minimize the training error and the norm of the output weights; a feature that according to Bartlett's theory will result in better generalizability of the model.

Therefore, the ELM objective function, which tries to minimize the training error and the norm of the output weights according to [43] is as follows.

$$\text{Minimize: } \|h\beta - T\|2 \text{ and } \|\beta,\| \tag{7}$$

where h is the hidden layer matrix and is given by:

$$H = \begin{bmatrix} h(x_1) \\ \dots \\ h(x_n) \end{bmatrix} = \begin{bmatrix} h_1(x_1) & \dots & h_L(x_1) \\ \dots & \dots & \dots \\ h_1(x_N) & \dots & h_L(x_N) \end{bmatrix}. \tag{8}$$

As can be seen, minimizing $\|\beta\|$ is, in fact, equivalent to maximizing the margin between the two classes in two-class classification, i.e., maximizing $\frac{2}{\|\beta\|}$.

Types of ELM models:

Single-output multi-class classification.
Multi-output multi-class classification.
In this study, we use the first type, single-output multi-class classification.

Since ELM can approximate any continuous function, one way for multi-class classification is to use an output that is close to the intended class in each area. In this case, the optimization problem according to [43] will be as follows.

$$\text{Minimize L Primal} - \text{ELM} = \frac{1}{2}\|B\|^2 + b^2 + C\frac{1}{2}\sum_{i=1}^{N} \varepsilon_i{}^2, \tag{9}$$

subject to: $h() = t_i - \xi i \; i = 1, \dots, N.$

2.7. Support Vector Regression

Support vector machine (SVM) is an improved machine learning algorithm, which could be used for regression and classification purposes. SVMs are mainly used in classification problems. In order to accept the error in the forecast, i.e., define the ε ratio, we need to present support vector machine with regression analysis, which is known as support vector regression. If we want to bound our error expectation to a certain degree, we can have the cost function for the soft margin hyperplane with constant C, based on [44,45], is as follows.

$$q(C) = \frac{1}{2}\|w\|^2 + C\frac{1}{N}\sum_{i=1}^{N} l_\varepsilon(y_i.\hat{y}_i), \tag{10}$$

where loss function $l_\varepsilon(y_i, \hat{y}_i)$, based on [44,45], is defined as follows.

$$l_\varepsilon(y_i, \hat{y}_i) = \begin{cases} |\hat{y}_{i-}y_i| - \varepsilon, & if |\hat{y}_{i-}y_i| \geq \varepsilon \\ 0 & otherwise \end{cases}, \tag{11}$$

where y_i is the real and $\hat{y}$ is the forecasted output of our model. This function decreases the forecast errors equal to or smaller than ε, and penalizes the values above ε by the amount of constant C, and adds the forecast error above ε to the cost function. In other words, the $l_\varepsilon(y_i, \hat{y}_i)$ function is indifferent to errors equal to or smaller than ε. With N training samples, the penalty function, which is the additional cost per each unit of error in the cost function of the problem, is defined as $C\frac{1}{N}\sum_{i=1}^{N} l_\varepsilon(y_i, \hat{y}_i)$ and known as empirical risk. So, using two slack variables $£_i$ and $£_i^*$ to add the surplus error, the optimization problem, based on [44,45], will be as follows.

$$Minimize \; \frac{1}{2}\|w\|^2 + C\sum_{i=1}^{N}\left(£_i + £_i^*\right), \tag{12}$$

$$subject \; to : y_i - w^T x_i - b \leq \varepsilon + £_i(1)$$
$$-y_i + w^T x_i + b \leq \varepsilon + £_i^*$$
$$£_i w £_i^* \geq 0.$$

Similar to the classification problem, the Lagrange function of the main problem is given by [46]:

$$\mathcal{L} = \frac{1}{2}\left(w^T w\right) + C\sum_{i=1}^{N}\left(£_i + £_i^*\right) - \sum_{i=1}^{N} \propto_i \left[-y_i + \left(w^t x_i\right) + b + \varepsilon + £_i\right]$$
$$- \sum_{i=1}^{N} \propto_i^* \left[y_i - \left(w^T x_i\right) - b + \varepsilon + £_i^*\right]. \tag{13}$$

Regarding the above problem, the constraints $£_i$ and $£_i^* \geq 0$ must be added to the Lagrangian model. Additionally, contrary to the classification case, there is no assumption as $\varepsilon = 1$, because in regression, {yi} determines the size of the problem. Now, taking the derivatives of the Lagrange function with respect to w, b, $£_i^*$ and $£_i$, we have [46]:

$$max - \frac{1}{2}\sum_{i=1}^{N}\sum_{j=1}^{N}\left(\propto_i - \propto_i^*\right)\left(\propto_j - \propto_j^*\right)\langle x_i, x_j\rangle - \varepsilon\sum_{i=1}^{N}\left(\propto_i + \propto_i^*\right) + \sum_{i=1}^{N} y_i\left(\propto_i - \propto_i^*\right), \tag{14}$$

$$subject \; to : \sum_{i=1}^{N}\left(\propto_i^* - \propto_i\right) = 0$$
$$0 \leq \propto_i \leq C$$
$$0 \leq \propto_i^* \leq C.$$

In the above problem, which should be optimized by changing $\propto_i$ and $\propto_i^*$ variables, $\left(\propto_i^* - \propto_i\right) \neq 0$ is the case in support vectors. Among support vectors, if $|\propto_i^* - \propto_i| = C$, the vector will fall out of the function range and is considered out of the acceptable region (ε region). Like the classification case, the kernel functions can substitute for $\langle x_i, x_j\rangle$ in the above function as well. The values for $\propto_i$ and $\propto_i^*$ are determined using quadratic programming to solve the problem. They are obtained with the equation $W = \sum_{i=1}^{N}\left(\propto_i - \propto_i^*\right)x_i$ for the coefficients matrix, which is made up of input data xi and is independent of the state variable y_i. To calculate b, the following equations can be used [46]:

$$b = y_i - \langle w, x_i\rangle - \varepsilon, \tag{15}$$

$$b = y_i - \langle w, x_i\rangle + \varepsilon. \tag{16}$$

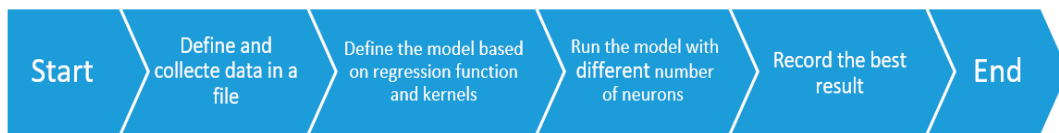Figure 4 illustrates the process of proposed model from start to stop.

Figure 4. Process of the proposed model.

2.8. The Functions Used in ELM

Some activation functions of the ELM model based on [47] are as follows.

"sig" stands for Sigmoidal function.
"sin" stands for Sine function.
"hardlim" stands for Hardlim function.
"tribas" stands for the trigonometric basis functions.

$$sigmoid\ function\ (a, b, x) = \frac{1}{1 + \exp(-(ax + b))} \tag{17}$$

Jahangir et al. [47] investigated the rainfall-runoff process simulation using a back propagation artificial neural network with a sigmoid activation function in Kardeh watershed. The results showed that a multilayer perceptron network with a hidden layer simulated the runoff process with high accuracy.

In this study, we use the Sigmoidal function in ELM to forecast the output energy.

2.9. Using Kernels

Kernels can also be used in ELM models, like the SVM-based models. In this case, the ELM kernel is defined as [48]:

$$\Omega ELM = HH^t : \Omega ELMi, = h(xi).h(xj) = K(xi, xj). \tag{18}$$

The output function of the model can be obtained with the kernel, as follows [48]:

$$f(x) = h(x)H^t\left(\frac{1}{C} + HH^t\right)^{-1}T = \begin{bmatrix} k(x, x_1) \\ k(x, x_n) \end{bmatrix}^T \left(\frac{1}{C} + \eta_{ELM}\right)^{-1}T \tag{19}$$

2.10. Performance Measures

The root mean square error (RMSE) measures the difference between values forecasted by a model or a statistical estimator and the actual values. RMSE is a good tool to compare the forecast errors made by a dataset [49–51]:

$$MSE = \frac{1}{n}\sum_{i=1}^{n}(\hat{y}_i - y_i)^2, \tag{20}$$

$$RMSE(\hat{\theta}) = \sqrt{MSE(\hat{\theta})} = \sqrt{E\left(\left(\hat{\theta} - \theta\right)^2\right)}, \tag{21}$$

$$R^2 = \frac{\sum d_i y_i - (\sum \frac{d_i y_i}{N})}{\sqrt{(\sum d_i^2 - (\sum d_i)^2 / (\sum y_i^2 - (\sum y_i)^2 / N)}}. \tag{22}$$

3. Results

3.1. The Pattern Used in Wheat Cultivation

Using the conversion factors presented in Table 4, the pattern for the energy consumption of each farm was studied. The average value of consumed energy from different sources and the total energy production are summarized in Table 4.

Table 4. Input energy.

Input	Unit	Average Consumed Energy	Percentage of Total Consumed Energy
Consumed water	m^3	10,638.60	14.568%
Chemical fertilizers			
Nitrogen	Kg	15,906.67	21.782%
Phosphate	Kg	1783.90	2.443%
Potassium	Kg	1873.20	2.565%
Pesticides			
Decis	Kg	43.740	0.060%
Carbendazim	Kg	235.200	0.322%
Pirimor	Kg	120.000	0.164%
Herbicide	Kg	172.80	0.237%
Labor	h	299.39	0.410%
Diesel fuel	L	27,772.23	38.031%
Equipment and machines	h	10,596.30	14.510%
Grain	Kg	3583.13	4.907%

In this study, the ELM and SVR methods are used as methods to forecast energy output to determine the best approach with the least forecast error. The accuracy and error of the model depend on the selected parameters (listed in Table 4). In this method, the accuracy of the model depends on the correct selection of the number of hidden layer neurons, as well as the amount of training data and testing data. The results obtained from the ELM and SVR model are shown in Table 5.

Table 5. Input and output energy table.

Input	Unit	Total Energy
Total input energy (consumed)	MJ	1,460,503.1
Output		
Output energy (produced wheat)	MJ	1,401,011.945

3.1.1. ELM Method

Figure 5 shows the plot of Quantile-Quantile (QQ) sample data versus standard normal and the dispersion around the regression line for the factors affecting input and output energy is shown in Figure 6. As can be seen, the plots are in a linear pattern. Clearly, the forecast at the training stage is better than the forecast at the testing stage. This indicates that the data for effective energy input parameters in the experiment section are irregular and insufficient. In the ELM method, 70% of the data are used as training and 30% of them are used as testing data. Additionally, the number of hidden neurons is 30, and the Sigmoidal kernel is used:

$$(\text{TrainResult}, \text{TestResult}') = \text{ELM\_V2}('\text{Nis}', 70, 0, 30, '\text{sig}'). \tag{23}$$
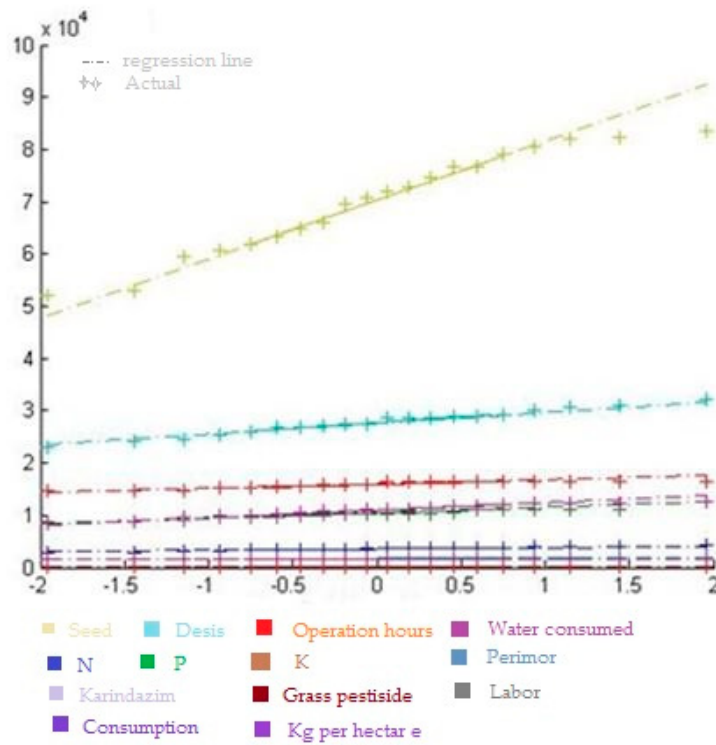
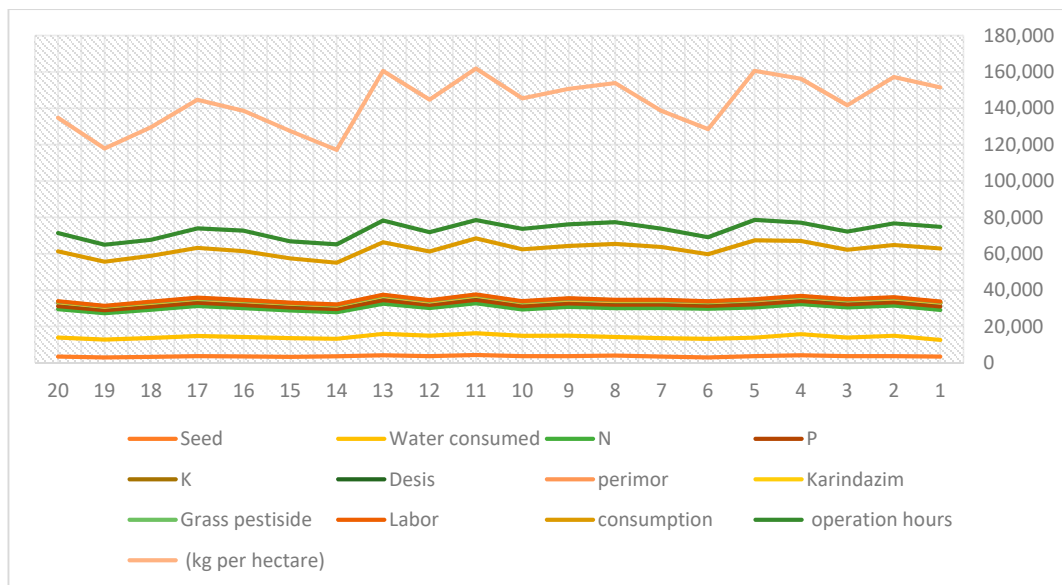**Figure 5.** Quantile-Quantile (QQ) plot of sample data versus standard normal.

Figure 6. Input and output energy charts.

3.1.2. Radial Basis SVR Method

Eleven neurons and radial basis function kernels in implementing the SVR method were utilized for this analysis. Figures 7–9 show the results for the training data stage, testing data stage, and all data, respectively.
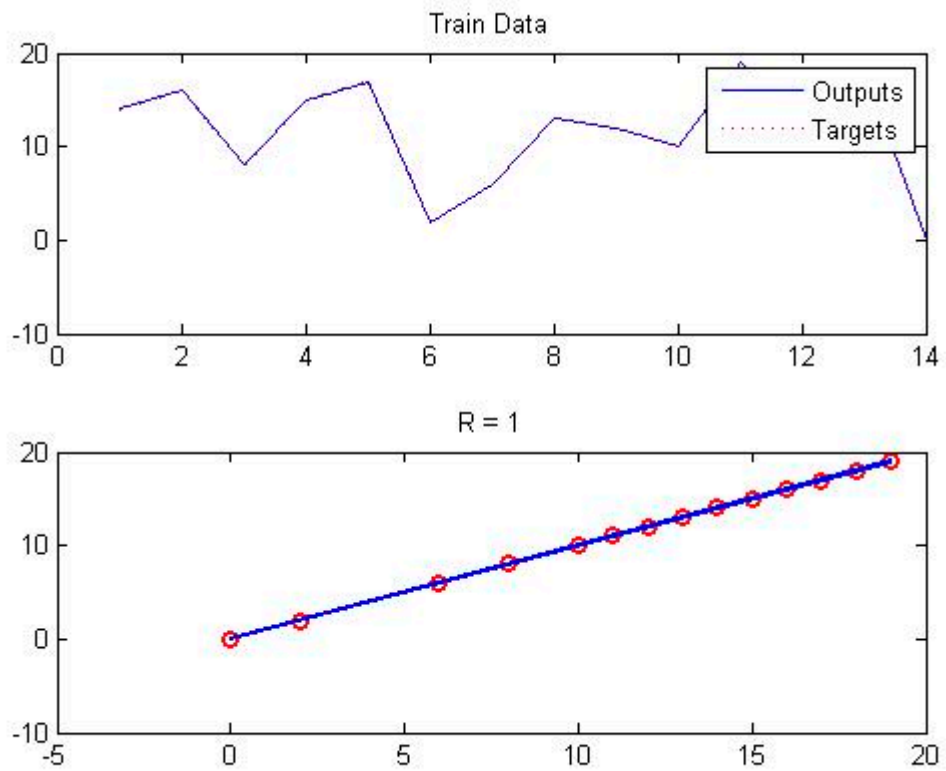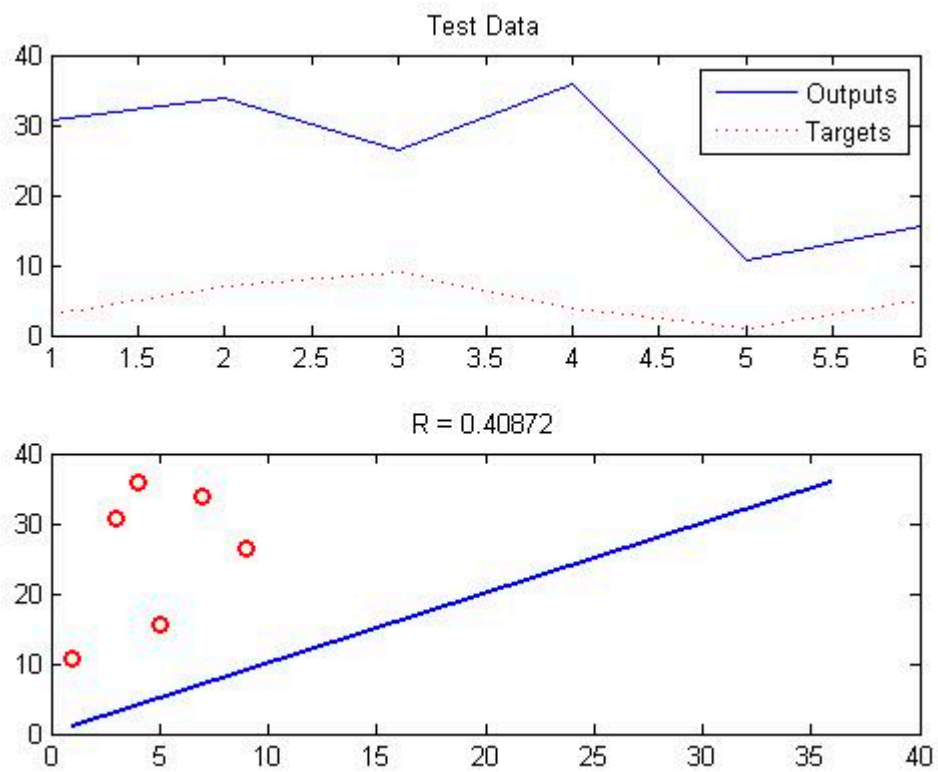
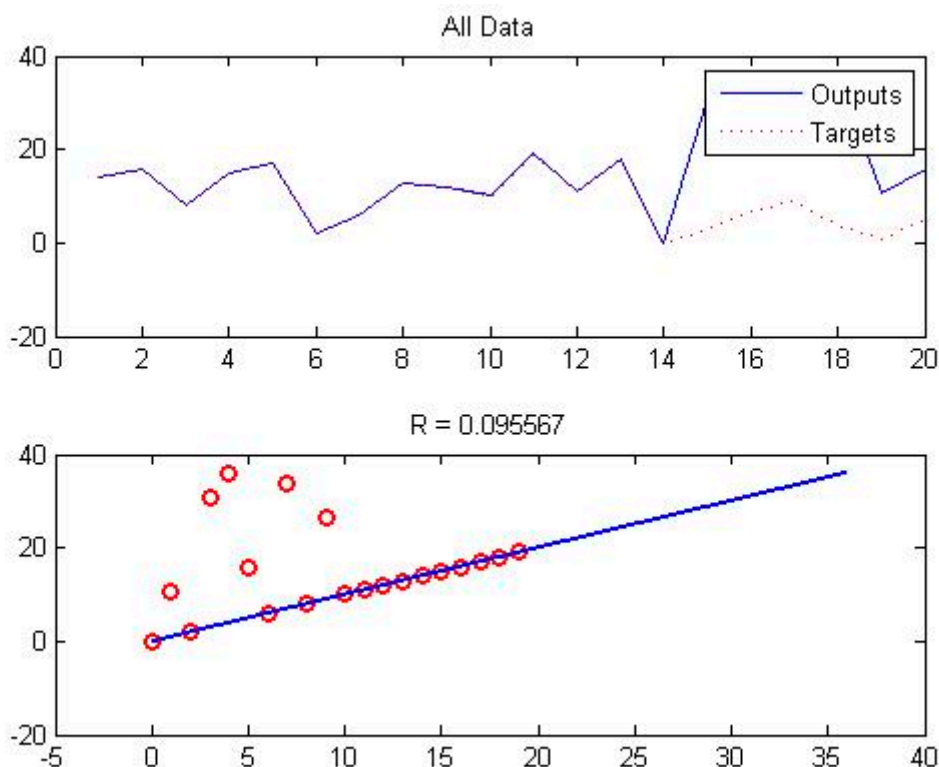**Figure 7.** Training data stage.

Figure 8. Testing data stage.

Figure 9. All data.

4. Discussion

The amount of energy input and output in the wheat fields was calculated to be 1,460,503.1 MJ and 1,401,011.945 MJ, respectively. The energy efficiency is 0.955653987%. According to Table 4, 37.888% of the total energy used is for diesel fuel, 21.7% for nitrogen fertilizer, 14.67% for machinery and equipment, and 14.653% for water, sorted by the amount of consumed energy. The results of the extreme learning machine (ELM) using the SVRrbf method are shown in Table 6.

Table 6. The results of Extreme Learning Machine (ELM) using the Support Vector Regression- Radial Basis Function (SVR-RBF) method.

Method	Train				Test			
	R^2	R	RMSE	MSE	R^2	R	RMSE	MSE
SVR	1	1	4.6088×10^{-12}	2.1241×10^{-23}	0.167052	0.40872	22.4384	503.4801
ELM	0.9623	0.981	0.0895	0.008	0.9531	0.9763	0.1010	0.0102

For performance measurement, we determined the relative importance of independent input parameters of ELM on the output. The root mean squared error (RMSE), correlation coefficient (R), R^2, and MSE were used to evaluate the difference between the ELM model's expected and actual values. R's value in the training stage of ELM is equal to 0.981, which is less than R = 1 in the SVR training stage. Additionally, in the testing stage of the ELM, R is 0.9763, which is larger than R = 0.40872 in the training of the SVR method. R in the testing stage of the ELM method is more significant than 0.8, so it is considered acceptable. The value of $R^2 = 0.9531$ in the ELM method's testing stage is greater than $R^2 = 0.167052$ of the SVR method and is therefore acceptable. The value of MSE = 0.0102 and RMSE = 0.01010 in the testing stage of ELM is much less than MSE = 503.4801 and RMSE = 22.4384 in the SVR method. The results of this study were gained within the Estahban region. The method of this study could be performed in other regions of the world and could also be used for other crops. Clearly, it could be used for other crops in which different data would be required.

Application of the Developed Model in the Future

The reason for studying the ELM and SVR methods is to develop an accurate forecasting model with minimal error, which can be utilized by policymakers and farmers in estimating the number of products at the end of the harvesting season. At the beginning of the planting season for wheat, farmers decide on how much of the cultivated fields should be allocated to wheat. This decision is made regarding the amount of annual precipitation and also, the amount of consumed water. Farmers are informed about the amount of consumed grain, chemical fertilizers, etc. due to experience and the region's views of agricultural engineers. They also have enough information to estimate and measure the materials required and the labor and machinery used. By correctly educating farmers on a large scale, they will be able to inform their local agricultural organizations about their product forecasts. This will help policymakers on deciding how much wheat should be imported, if necessary at all. Additionally, this can have a significant impact on the appropriate pricing of wheat, in order to protect farmers and the community. Another advantage of this model includes using farmers' forecasted data to propose a dynamic model of the agricultural system, simulating future data, estimating the amount of product and materials to be consumed in the future, making decisions, and preventing future risk factors.

5. Conclusions

Energy consumption has a significant impact on global warming and climate change. So reducing energy consumption will have a great effect on controlling the increasing rate of global warming. With regard to the data in Table 4, one can infer that to reduce the amount of energy consumption in wheat production, it is possible to limit the amount of nitrogen fertilizer, diesel fuel, and water, and also utilize more energy-efficient machinery and equipment. In this study, extreme learning machine and support vector regression methods were applied to forecast wheat production's output energy in the Estahban region. The data for agricultural parameters effective in the production of wheat were converted into their energy equivalent and used as the model's inputs. The results showed that ELM is better than SVR and other methods for forecasting wheat production's output energy in Estahban. Furthermore, the ELM method has much smaller error than radial basis function SVR and can provide more accurate forecasts. It also is faster than the SVR method for forecasting problems. The extended ELM model is capable of learning patterns and can forecast the model's energy output with the lowest error. The ELM method can be used to forecast other agricultural products. The results showed that the proposed method is able to improve forecast accuracy and can be generalized. So, ELM can be an excellent alternative to radial basis function SVR. The concluding remarks are as follows.

- To produce wheat in Estahban, 1,460,503.1 MJ of energy is required.
- From the obtained data, it is not energy efficient to produce wheat because 1,460,503.1 MJ energy is required to produce it, the total energy of which is 1,401,011.9 MJ. On the other hand, wheat is necessary for human beings.
- The extreme ELM model is capable of learning patterns and can forecast the energy output of the model with the lowest error.

In the future, researchers could use different crops to predict the required energy. Additionally, other countries could be investigated for this purpose. Finally, different methods and algorithms can also be used and compared.

Conflicts of Interest: The authors declare no conflict of interest.

References

1. Ewel, J.J.; Schreeg, L.A.; Sinclair, T.R. Resources for crop production: Accessing the unavailable. *Trends Plant Sci.* **2019**, *24*, 121–129. [CrossRef] [PubMed]

2. Walls, H.; Baker, P.; Chirwa, E.; Hawkins, B. Food security, food safety & healthy nutrition: Are they compatible? *Glob. Food Secur.* **2019**, *21*, 69–71.

3. Sakizadeh, M.; Zhang, C. Health risk assessment of nitrate using a probabilistic approach in groundwater resources of western part of Iran. *Environ. Earth Sci.* **2020**, *79*, 43. [CrossRef]

4. Hosseinzadeh-Bandbafha, H.; Safarzadeh, D.; Ahmadi, E.; Nabavi-Pelesaraei, A. Optimization of energy consumption of dairy farms using data envelopment analysis—A case study: Qazvin city of Iran. *J. Saudi Soc. Agric. Sci.* **2018**, *17*, 217–228. [CrossRef]

5. Rajabi, M.H.; Soltani, A.; Zeynali, E.; Soltani, E. Evaluation of Energy Use in Wheat Production in Gorgan. *J. Plant Prod. (J. Agric. Sci. Nat. Resour.)* **2012**, *19*, 143–171.

6. Global Wheat Crop Condition Mostly Favorable: AMIS. Available online: https://www.graincentral.com/markets/global-wheat-crop-condition-mostly-favourable-amis/ (accessed on 14 July 2019).

7. World Wheat Crop Set for Rebound: AMIS. Available online: https://www.graincentral.com/markets/world-wheat-crop-set-for-rebound-amis/ (accessed on 14 July 2019).

8. Agricultural Statistics for 2015–2016 Crop Year. Available online: https://www.maj.ir/Dorsapax/userfiles/Sub65/Amarnamehj193-94.pdf (accessed on 24 October 2019).

9. Commodity Intelligence Report. Available online: https://ipad.fas.usda.gov/highlights/2008/05/Iran_may2008.htm (accessed on 17 November 2019).

10. Focus on Iran. Available online: https://www.world-grain.com/articles/12752-focus-on-iran (accessed on 17 November 2019).

11. GIEWS-Global Information and Early Warning System. Available online: http://www.fao.org/giews/countrybrief/country.jsp%3Fcode%3DIRN (accessed on 17 November 2019).

12. Taki, M.; Mahmoudi, A.; Mobtaker, H.G.; Rahbari, H. Energy consumption and modeling of output energy with multilayer feed-forward neural network for corn silage in Iran. *Agric. Eng. Int. CIGR J.* **2012**, *14*, 93–101.

13. Bansal, S.; Roy, S.; Larachi, F. Support vector regression models for trickle bed reactors. *Chem. Eng. J.* **2012**, *207*, 822–831. [CrossRef]

14. Mitchell, T.M. *Machine Learning*; McGraw Hill: Burr Ridge, IL, USA, 1997; Volume 45, pp. 870–877.

15. Memon, M.I.; Noonari, S.; Laghari, M.A.; Pathan, M.; Pathan, A.; Sial, S.A. Energy Consumption Pattern in Wheat Production in Sindh Pakistan. *Energy* **2015**, *5*, 63–77.

16. Zangeneh, M.; Omid, M.; Akram, A. A comparative study on energy use and cost analysis of potato production under different farming technologies in Hamadan province of Iran. *Energy* **2010**, *35*, 2927–2933. [CrossRef]

17. He, Q.; Jin, X.; Du, C.; Zhuang, F.; Shi, Z. Clustering in extreme learning machine feature space. *Neurocomputing* **2014**, *128*, 88–95. [CrossRef]

18. Lei, Y.; Zhao, D.; Cai, H. Prediction of length-of-day using extreme learning machine. *Geod. Geodyn.* **2015**, *6*, 151–159. [CrossRef]

19. Neumann, K.; Rolf, M.; Steil, J.J. Reliable integration of continuous constraints into extreme learning machines. *Int. J. Uncertain. Fuzziness Knowl. Based Syst.* **2013**, *21* (Suppl. S02), 35–50. [CrossRef]

20. Nath, B.; Dhakre, D.S.; Bhattacharya, D. Forecasting wheat production in India: An ARIMA modelling approach. *J. Pharmacogn. Phytochem.* **2019**, *8*, 2158–2165.

21. Haider, S.A.; Naqvi, S.R.; Akram, T.; Umar, G.A.; Shahzad, A.; Sial, M.R.; Khaliq, S.; Kamran, M. LSTM neural network based forecasting model for wheat production in Pakistan. *Agronomy* **2019**, *9*, 72. [CrossRef]

22. Santamaría-Artigas, A.E.; Franch, B.; Guillevic, P.; Roger, J.C.; Vermote, E.F.; Skakun, S. Evaluation of Near-Surface Air Temperature From Reanalysis Over the United States and Ukraine: Application to Winter Wheat Yield Forecasting. *IEEE J. Sel. Top. Appl. Earth Obs. Remote Sens.* **2019**, *12*, 2260–2269. [CrossRef]

23. Shelia, V.; Hansen, J.; Sharda, V.; Porter, C.; Aggarwal, P.; Wilkerson, C.J.; Hoogenboom, G. A multi-scale and multi-model gridded framework for forecasting crop production, risk analysis, and climate change impact studies. *Environ. Model. Softw.* **2019**, *115*, 144–154. [CrossRef]

24. Yazdani, M. The Economic and Statistical Evaluation of Climatic Elements in Tabriz and Isfahan (in Iran). *J. Bus. Manag. Econ. Res.* **2019**, *3*, 18. [CrossRef]

25. Ram, B.; Rashid, M.; Lakhwani, K.; Kumar, S.S. Health Detection of Wheat Crop Using Pattern Recognition and Image Processing. *Int. J. Healthc. Inf. Syst. Inform. (IJHISI)* **2020**, *15*, 50–60. [CrossRef]

26. Ali, M.; Deo, R.C. Modeling wheat yield with data-intelligent algorithms: Artificial neural network versus genetic programming and minimax probability machine regression. In *Handbook of Probabilistic Models*; Butterworth-Heinemann: Waltham, MA, USA, 2020; pp. 37–87.

27. Salim, N.; Raza, A. Nutrient use efficiency (NUE) for sustainable wheat production: A review. *J. Plant Nutr.* **2020**, *43*, 297–315. [CrossRef]

28. Kamir, E.; Waldner, F.; Hochman, Z. Estimating wheat yields in Australia using climate records, satellite image time series and machine learning methods. *ISPRS J. Photogramm. Remote Sens.* **2020**, *160*, 124–135. [CrossRef]

29. Pantazi, X.E.; Moshou, D.; Alexandridis, T.; Whetton, R.L.; Mouazen, A.M. Wheat yield prediction using machine learning and advanced sensing techniques. *Comput. Electron. Agric.* **2016**, *121*, 57–65. [CrossRef]

30. Amato, F.; Castiglione, A.; Moscato, V.; Picariello, A.; Sperli, G. Multimedia summarization using social media content. *Multimed. Tools Appl.* **2018**, *77*, 17803–17827. [CrossRef]

31. Wang, D.; Zhan, Y.; Yu, T.; Liu, Y.; Jin, X.; Ren, X.; Chen, X.; Liu, Q. Improving Meteorological Input for Surface Energy Balance System Utilizing Mesoscale Weather Research and Forecasting Model for Estimating Daily Actual Evapotranspiration. *Water* **2020**, *12*, 9. [CrossRef]

32. Yousefi, M.; Khoshnevisan, B.; Shamshirband, S.; Motamedi, S.; Nasir, M.H.; Arif, M.; Ahmad, R. Support vector regression methodology for prediction of output energy in rice production. *Stoch. Environ. Res. Risk Assess.* **2015**, *29*, 2115–2126. [CrossRef]

33. Acaroğlu, M.; Aksoy, A.Ş. The cultivation and energy balance of Miscanthus× giganteus production in Turkey. *Biomass Bioenergy* **2005**, *29*, 42–48. [CrossRef]

34. Esengun, K.; Erdal, G.; Gündüz, O.; Erdal, H. An economic analysis and energy use in stake-tomato production in Tokat province of Turkey. *Renew. Energy* **2007**, *32*, 1873–1881. [CrossRef]

35. Singh, J.M. On Farm Energy Use Pattern in Different Cropping Systems in Haryana, India. Master's Thesis, International Institute of Management, University of Flensburg, Flensburg, Germany, 2002.

36. Canakci, M.; Topakci, M.; Akinci, I.; Ozmerzi, A. Energy use pattern of some field crops and vegetable production: Case study for Antalya Region, Turkey. *Energy Convers. Manag.* **2005**, *46*, 655–666. [CrossRef]

37. Ozkan, B.; Akcaoz, H.; Fert, C. Energy input–output analysis in Turkish agriculture. *Renew. Energy* **2004**, *29*, 39–51. [CrossRef]

38. Erdal, G.; Esengün, K.; Erdal, H.; Gündüz, O. Energy use and economical analysis of sugar beet production in Tokat province of Turkey. *Energy* **2007**, *32*, 35–41. [CrossRef]

39. Ozkan, B.; Akcaoz, H.; Karadeniz, F. Energy requirement and economic analysis of citrus production in Turkey. *Energy Convers. Manag.* **2004**, *45*, 1821–1830. [CrossRef]

40. Deng, W.; Zheng, Q.; Chen, L. Regularized extreme learning machine. In *2009 IEEE Symposium on Computational Intelligence and Data Mining*; IEEE: New York City, NY, USA, 2009; pp. 389–395.

41. Huang, G.B.; Bai, Z.; Kasun, L.L.; Vong, C.M. Local receptive fields based extreme learning machine. *IEEE Comput. Intell. Mag.* **2015**, *10*, 18–29. [CrossRef]

42. Kasun, L.L.; Yang, Y.; Huang, G.B.; Zhang, Z. Dimension reduction with extreme learning machine. *IEEE Trans. Image Process.* **2016**, *25*, 3906–3918. [CrossRef]

43. Huang, G.B.; Zhou, H.; Ding, X.; Zhang, R. Extreme learning machine for regression and multiclass classification. *IEEE Trans. Syst. Man Cybern. Part B* **2012**, *42*, 513–529. [CrossRef]

44. Alamili, M. *Exchange Rate Prediction Using Support Vector Machines*; Technische Universiteit Delft: Delft, The Netherlands, 2011.

45. Smola, A.J.; Schölkopf, B. A tutorial on support vector regression. *Stat. Comput.* **2004**, *14*, 199–222. [CrossRef]

46. Welling, M. *Support Vector Regression*; Department of Computer Science, University of Toronto: Toronto, ON, Canada, 2004.

47. Jahangir, A.; Raeini, S.M.; Ziatabar, A.M. Comparison of artificial neural networks (ANN) simulation of rainfall-runoff process with HEC-HMS model in Kardeh watershed. *J. Soil Water Conserv.* **2008**, *2*, 72–84.

48. Miche, Y.; Sorjamaa, A.; Bas, P.; Simula, O.; Jutten, C.; Lendasse, A. OP-ELM: Optimally pruned extreme learning machine. *IEEE Trans. Neural Netw.* **2010**, *21*, 158–162. [CrossRef]

49. Panahi, M.; Gayen, A.; Pourghasemi, H.R.; Rezaie, F.; Lee, S. Spatial prediction of landslide susceptibility using hybrid support vector regression (SVR) and the adaptive neuro-fuzzy inference system (ANFIS) with various metaheuristic algorithms. *Sci. Total Environ.* **2020**, *741*, 139937. [CrossRef]

50. Samadianfard, S.; Hashemi, S.; Kargar, K.; Izadyar, M.; Mostafaeipour, A.; Mosavi, A.; Nabipour, N.; Shamshirband, S. Wind speed prediction using a hybrid model of the multi-layer perceptron and whale optimization algorithm. *Energy Rep. Energy Rep.* **2020**, *6*, 1147–1159. [CrossRef]

51. Mostafaeipour, A.; Goli, A.; Qolipour, M. Prediction of air travel demand using a hybrid artificial neural network (ANN) with Bat and Firefly algorithms: A case study. *J. Supercomput.* **2018**, *74*, 5461–5484. [CrossRef]

Publisher's Note: MDPI stays neutral with regard to jurisdictional claims in published maps and institutional affiliations.